

# Tunable Triple-Notched Ultra-Wideband Bandpass Filter for Efficient In-Band and Out-of-Band Interference Mitigation

Richard Patience Shema<sup>1</sup> , Dominic B. O. Konditi<sup>2</sup>,  and Elijah Mwangi<sup>3</sup> 

<sup>1</sup>Department of Electrical Engineering, Pan African University Institute for Basic Sciences, Technology and Innovation (PAUSTI) hosted within Jomo Kenyatta University of Agriculture and Technology (JKUAT), Nairobi, Kenya, [patience.richard@students.jkuat.ac.ke](mailto:patience.richard@students.jkuat.ac.ke)

<sup>2</sup>School of Electrical and Electronic Engineering, Technical University of Kenya, Nairobi, Kenya, [dominic.konditi@tukenya.ac.ke](mailto:dominic.konditi@tukenya.ac.ke)

<sup>3</sup>Department of Electrical and Information Engineering, University of Nairobi, Nairobi, Kenya, [elijah.mwangi@uonbi.ac.ke](mailto:elijah.mwangi@uonbi.ac.ke)

\*Correspondence: [patience.richard@students.jkuat.ac.ke](mailto:patience.richard@students.jkuat.ac.ke)

**ABSTRACT-** This study analyzes the growing need for effective in-band and out-of-band interference mitigation in ultra-wideband (UWB) communication systems. We present a novel microstrip bandpass filter (BPF) with changeable triple-notched bands that preserves a large passband and a higher stopband. The filter comprises a multimode resonator (MMR) architecture that incorporates a hollow T-shaped structure that generates two transmission zeros at the passband boundaries, thereby boosting selectivity. Furthermore, we deploy a circular complementary split-ring resonator (CCSRR)-based metamaterial to extend the upper stopband and implement a folded  $\Xi$ -shaped electromagnetic bandgap (EBG) architecture for dynamic notch frequency modulation. This design achieves sharp notches at 4.93 GHz, 6.32 GHz, and 9.81 GHz, efficiently minimizing the interference from WLAN and X-band satellite signals. The simulation results revealed a passband ranging from 3.06 to 10.79 GHz, with an insertion loss of less than 1.2 dB and a relative bandwidth of 112.85%. The filter exhibits significant selectivity, including a skirt factor of 0.91 and an upper stopband reaching 19.8 GHz with an insertion loss of 18 dB, rendering it suitable for UWB applications that require substantial interference rejection.

**Keywords:** Ultra-wideband (UWB), Triple Notched Bands, Bandpass Filter (BPF), Interference Mitigation, Metamaterial.

## ARTICLE INFORMATION

**Author(s):** Richard Patience Shema, Dominic B.O. Konditi, Elijah Mwangi;

**Received:** 17/10/2024; **Accepted:** 15/03/2025; **Published:** 20/06/2025;

**E- ISSN:** 2347-470X;

**Paper Id:** IJEER240428;

**Citation:** 10.37391/ijeer.130214

**Webpage-link:**

<https://ijeer.forexjournal.co.in/archive/volume-13/ijeer-130214.html>

**Publisher's Note:** FOREX Publication stays neutral with regard to jurisdictional claims in Published maps and institutional affiliations.



## 1. INTRODUCTION

Ultra-wideband (UWB) technology has attracted substantial attention throughout the past decade owing to its potential for high-speed communication across wireless networks, security systems, and applications requiring imaging [1]. UWB systems operate in a large frequency range, particularly from 3.1 GHz to 10.6 GHz, enabling a high bandwidth for data transmission [2]. However, enabling good signal transmission throughout this broad spectrum involves various problems, particularly interference from the bordering frequency bands and ensuring sufficient selectivity. One of the key components of UWB structures is a bandpass filter (BPF), which has a vital function in signal shaping and noise rejection. The design of BPFs for UWB applications requires careful consideration of performance aspects, including selectivity, return loss, insertion

loss, and the capacity to manage in-band and out-of-band interference. Moreover, the presence of undesired signals inside the UWB spectrum, such as those from WLAN, WiMAX, C-band, and X-band satellite communications, requires the implementation of notch bands to prevent signal interference [3].

Various notch-band UWB bandpass filters have been proposed to mitigate the interference caused by narrowband systems in ultra-wideband systems. Many notch techniques have been proposed for UWB-bandpass filters. In [4]–[6], a notch was generated by etching a defected ground structure (DGS) into a multimode resonator (MMR) structure. In [4], three rectangular defected ground structures etched on the ground plane were used to mitigate the three interfering frequency bands in C, X, and fixed wireless systems. In [6], a single notch band characteristic was obtained by incorporating hybrid DGS techniques, that is, a combination of a spiral-shaped resonator and an H-slot resonator in the ground plane. Nevertheless, this approach of incorporating notches is not appropriate for the implementation of several notch bands with sharp selectivity. In [7]–[9], a notch band was implemented using line slots. In [7], a meander line slot was designed to avoid interference from WLAN signals, and in [9], a spiral slot was studied and adopted to introduce a notched band. However, the selectivity of the filter is very low. In [10], by placing open stubs in microstrips, the filter realizes a notched band in the passband; in [11], the process of creating a notch band is explained using concepts

related to transversal signal interactions; in [12], three notches were created by implementing a comb-like resonator configuration beneath the uniform impedance resonator and symmetrically expanding the bottom arm edge of the interdigital coupled lines; and in [13], a triple-notch ultrawideband filter utilizing an Archimedean spiral electromagnetic bandgap configuration was introduced, these above mentioned designs suffer either from poor transmission coefficients within the notches, poor upper stopband performance, or larger circuitry size.

To address these issues, this study presents a novel microstrip bandpass filter for UWB applications. The novelty of this study lies in its integrated approach to the UWB filter design. Specifically, it introduces a novel microstrip bandpass filter that uniquely combines a hollow T-shaped stub with a multimode resonator to generate two precise transmission zeros, thereby significantly enhancing the selectivity at the passband edges. Additionally, this study innovatively extends the upper stopband by incorporating circular complementary split-ring resonators (CCSRR), a strategy that effectively minimizes interference from neighboring frequency bands. Furthermore, the design integrates a folded  $\Xi$ -shaped electromagnetic bandgap (EBG) structure, which uniquely enables the formation of three tunable notched bands to suppress narrowband interference from systems such as WLAN and X-band satellite communication. Together, these integrated design elements deliver a compact, high-performance filter with a wide passband, low insertion loss, and excellent interference mitigation, representing a significant advancement over the existing UWB filter solutions.

The remainder of this study is organized into 5 sections. *Section 2* details the synthesis of the UWB bandpass filter, focusing on the design of the multimode resonator with a hollow T-shaped stub that generates key transmission zeros for enhanced selectivity. In *section 3*, the integration of the folded  $\Xi$ -shaped electromagnetic bandgap (EBG) architecture is presented, explaining how its triple-mode resonant features enable the formation of tunable notched bands for effective interference-mitigation. *Section 4* discusses the simulation results and performance evaluation, highlighting the filter's operational bandwidth, insertion loss, and upper stopband characteristics. Finally, *Section 5* summarizes the conclusions and potential implications of the proposed design for advanced UWB communication systems.

## 2. UWB BANDPASS FILTER SYNTHESIS

The filter presented in this study consists primarily of a multimode resonator composed of a step-impedance transmission line. To achieve optimal selectivity, a hollow T-shaped structure was connected in parallel at its center to provide transmission zeros. This structure generates transmission zeros on either side of the passband, thereby enhancing the filter's selectivity. The model of the improved filter is illustrated in *figure 1 (a)*, whereas *figure 1 (b)* presents an equivalent model of the MMR structure with a hollow T-shaped structure.

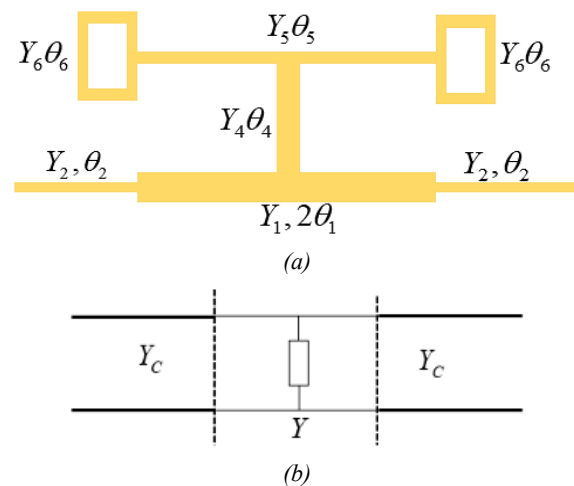


**Figure 1.** Hollow T-shaped UWB BPF (a) the configuration (b) the equivalent model

According to [14] and as illustrated in *figure 1 (b)*, its scattering parameters can be expressed as

$$\frac{1}{2 + \bar{Y}} \begin{bmatrix} -\bar{Y} & 2 \\ 2 & -\bar{Y} \end{bmatrix} \quad (1)$$

$$\bar{Y} = \frac{Y}{Y_c} \quad (2)$$

Where,

$$Y = Y_4 \frac{Y_{in1} + jY_2 \tan \theta_4}{Y_2 + jY_{in1} \tan \theta_4} \quad (3)$$

$$Y_{in1} = 2jY_5 \frac{Y_6 \tan \theta_6 + Y_5 \tan \theta_5}{Y_5 - Y_6 \tan \theta_5 \tan \theta_6} \quad (4)$$

From *equation (1)*, it can be deduced that  $S_{21} = 2/(1+Y)$ . By setting  $S_{21} = 0$ , the conditions for the occurrence of transmission zeroes can be determined as

$$Y_5 - Y_6 \tan \theta_6 \tan \theta_5 = 0 \quad (5)$$

$$\tan \theta_4 = 0 \quad (6)$$

where  $k = Y_6/Y_5$  and  $\theta = \theta_5 = \theta_6$  when  $\theta_4 = \pi/2$ ,  $f_{TZ1}$  is the first transmission zero at the lower band of the passband, and  $f_{TZ2}$  is the second transmission zero at the upper band of the passband, which can be obtained as

$$\theta(f_{TZ1}) = \arctan\left(\sqrt{1/k}\right) \quad (7)$$

$$\theta(f_{TZ2}) = \pi - \arctan\left(\sqrt{1/k}\right) \quad (8)$$

The above equations demonstrate that the transmission zeros,  $f_{TZ1}$  and  $f_{TZ2}$ , are jointly influenced by the admittance ratio  $k$  and the lengths  $L_5$  and  $L_6$ .

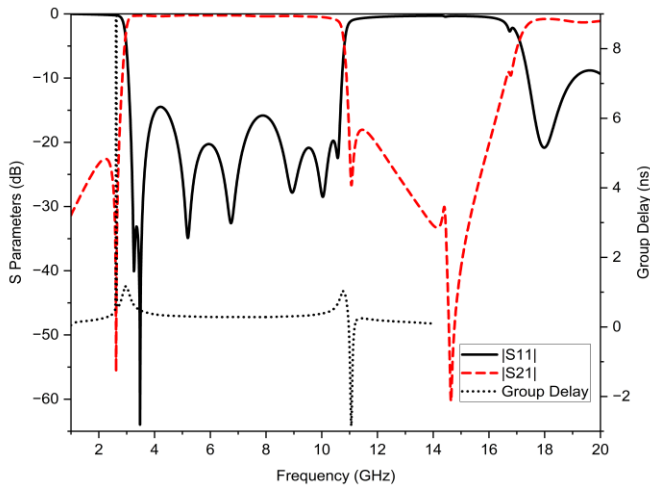


**Figure 2.** S-Parameters Hollow T-shaped UWB BPF

By conducting an optimization analysis of the admittance ratio  $k$  and lengths  $L_5$  and  $L_6$ , the S-parameters for the highly selective UWB BPF, as shown in *figure 2*, were obtained. In this figure, the transmission zeros  $f_{TZ1}$  and  $f_{TZ2}$  occur at 2.63 GHz and 11.07 GHz, respectively, with a -25 dB skirt factor of 0.93. These results clearly demonstrate that the introduction of hollow T-shaped stubs effectively enhances the filter selectivity by generating transmission zeros. The filter has a 3dB bandwidth extend from 2.97 GHz to 10.76 GHz, a relative bandwidth of 113.72%, a steady group delay of 0.3 ns in the passband and the upper stopband is from 10.98 GHz to 16.15 GHz with S21 of 17.9dB. The filter's size is  $0.26 \lambda_g \times 0.99 \lambda_g$ ;  $\lambda_g$  as the wavelength in the dielectric at the center frequency of 6.85 GHz, and its dimensions are given in *table 1*.

**Table 1. Dimensions of Hollow T-shaped UWB BPF (all values in mm)**

Parameter	Value	Parameter	Value	Parameter	Value
L0	8.1	L3	8.2	L6	4.39
W0	1.64	W3	0.21	W6	2.14
L1	15.21	L4	3.87	t6	0.55
W1	2.15	W4	1.11	S	0.1
L2	8.26	L5	11.76	g	0.28
W2	0.25	W5	0.55		

Studies indicate that a complementary split-ring resonator (CSRR) positioned on the ground plane or conductor strip demonstrates negative effective permittivity at its resonant frequencies [15], [16]. Consequently, the CSRR unit, characterized by inductive and capacitive components arranged in parallel, can be defined as a resonant circuit with a resonant frequency expressed as follows [17]:

$$f_r = \frac{1}{2\pi\sqrt{L_o C_c}} \quad (9)$$

$L_o$  denotes the equivalent inductance, whereas  $C_c$  signifies the equivalent capacitance of the CSRR.

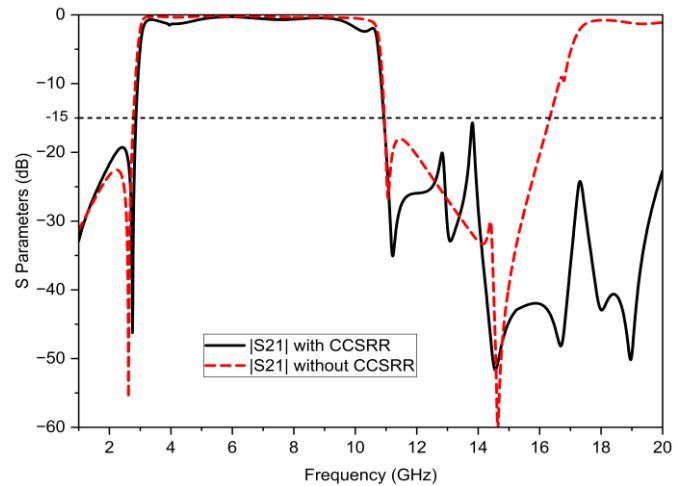


**Figure 3.** Simulated S21 with and without CCSRR structure

To attain an enhanced out-of-band performance, two pairs of circular complementary split-ring resonator (CCSRR)-based metamaterials were integrated into the ground plane beneath the center part of the MMR in the UWB filter. Cross-coupling has been established between two neighboring CCSRR stubs, resulting in the generation of additional transmission zeros in the upper stopband, thereby successfully mitigating undesirable spurious frequency bands. *Figure 3* shows the simulated transmission coefficients (S21) with and without the CCSRR. As shown in this figure, the upper stopband was extended from 10.94 GHz to 20 GHz with more than 15 dB of attenuation, where most of the part is below 20 dB.

### 3. NOTCHED-BAND UWB BPF SYNTHESIS

To mitigate interference from narrowband systems in ultra-wideband (UWB) systems, three tunable notch bands are incorporated into the UWB bandpass filter to mitigate interference from narrowband systems in UWB systems. These notch bands are introduced by coupling a folded  $\Xi$ -shaped electromagnetic bandgap (EBG) architecture unit in proximity to the multimode resonator (MMR) of the basic UWB filter.

#### 3.1 Folded EBG Architecture Analysis

The folded  $\Xi$ -shaped EBG architecture demonstrates three separate resonance frequencies and gives a significant degree of tuning flexibility. It was folded to lessen the capacitive couplings between the two resonators at the end and to achieve a compact size. The analysis demonstrates that its triple-mode resonant features permit the fabrication of a triple-band stop performance. These three notched bands can be easily created and fine-tuned by altering the resonance frequencies of the even and odd modes within the EBG structure, which contains two half-wavelength resonators and two short-circuit stubs positioned in the central plane. Owing to the symmetrical structure of the resonator, the odd-even-mode analysis method can be performed, and the resonant frequencies can be determined [18]. The odd-mode resonant frequency is determined as follows:

$$f_{in,odd} = \frac{c}{4L_{a1}\sqrt{\epsilon_{eff}}} \quad (10)$$

where  $f_{in}$  is the notch band central frequency,  $c$  is the speed of light in a vacuum, and  $\epsilon_{eff}$  is the effective dielectric constant.

The resonant frequencies of the even mode can be calculated as follows:

$$f_{in,even1} = \frac{c}{4(L_{a1} + L_{a2} + L_{a3})\sqrt{\epsilon_{eff}}} \quad (11)$$

$$f_{in,even2} = \frac{c}{2(L_{a1} + L_{a2} + L_{a4})\sqrt{\epsilon_{eff}}} \quad (12)$$

From the above equations, the resonance frequencies can be established based on the electrical length. Furthermore, the proposed structure can generate three resonant frequencies, providing greater freedom to modify the placement of the resonant modes. The suggested  $\Xi$ -shaped EBG can accomplish triple band-stop functionality when positioned adjacent to the microstrip line, effectively operating as three shunt-connected series resonance circuits, as depicted in *figure 4*.

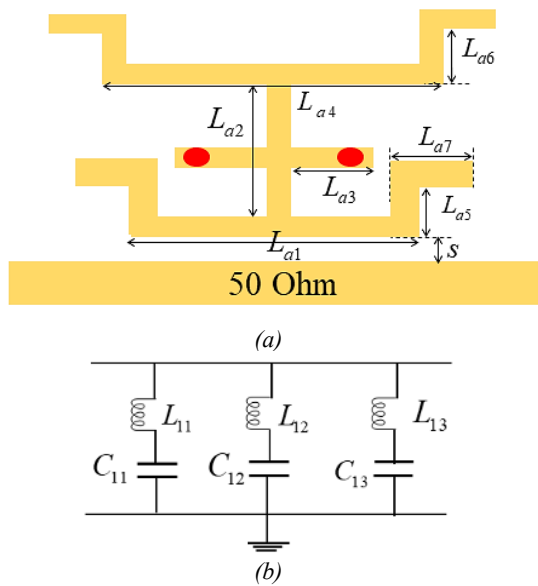


**Figure 4.** Structure of the EBG (a) the test model with a  $50 \Omega$  microstrip line (b) its equivalent model

The frequency characteristics of the linked EBG of various dimensions were investigated using HFSS software to confirm its multimode resonant behavior, as shown in *figure 5*. The results indicate that increasing the lengths of  $L_{a2}$  and  $L_{a4}$  causes the frequency locations of the first and second notched bands to simultaneously decrease downward. Comparatively, increasing  $L_{a1}$  leads to a decrease in the second and third notched bands. However, diminishing  $L_{a3}$  causes only the first notched band to move upwards. Therefore, by carefully modifying the resonator dimensions, it is feasible to generate three adjustable notched bands at the required frequencies.

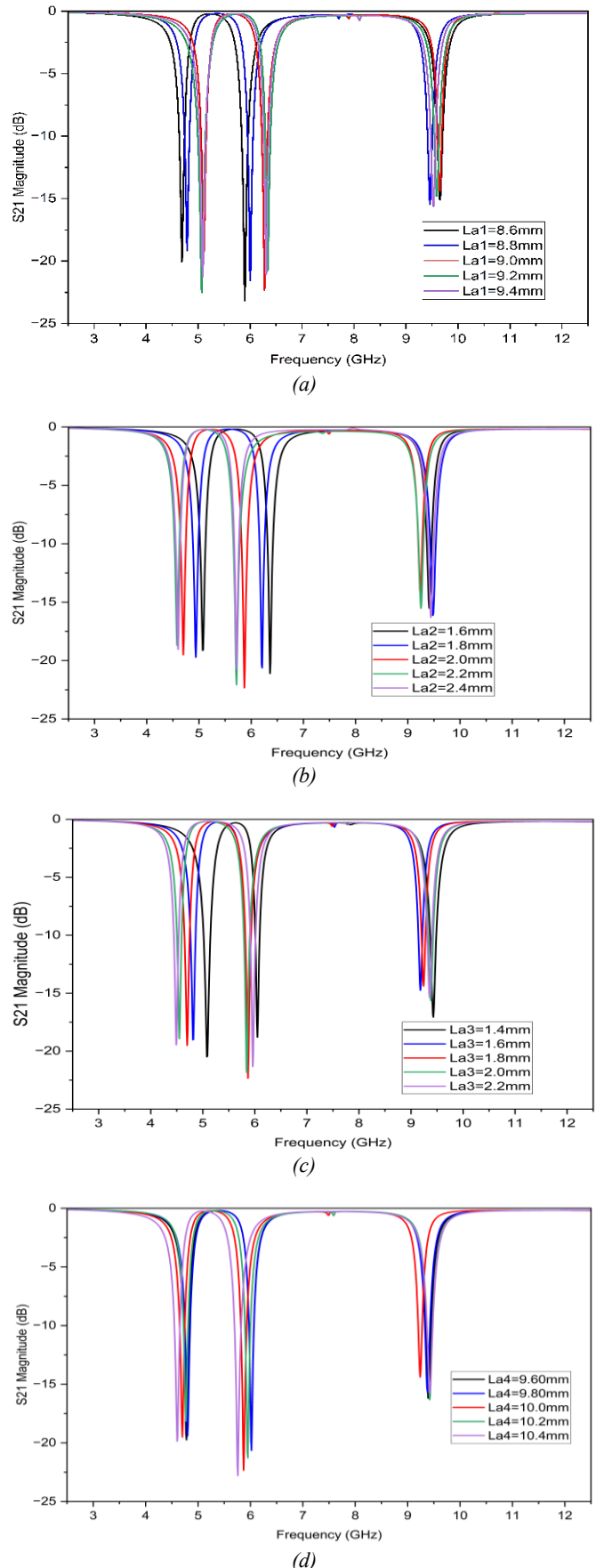


**Figure 5.** Simulated S-Parameters of the coupled folded EBG for different dimensions (a)  $L_{a1}$ , (b)  $L_{a2}$ , (c)  $L_{a3}$ , and (d)  $L_{a4}$

### 3.2 Triple Notched Band UWB Filter Analysis

Figure 6 displays the placement of the folded  $\Xi$ -shaped EBG unit near the fundamental hollow T-shaped stub-loaded MMR filter to generate triple-notched bands within the UWB passband; Figure 6 (a) shows the top layer and (b) shows the bottom layer displaying the CCSSR placement. The coupling gap (S) was determined to be the lowest possible distance to optimize the coupling between the EBG and the fundamental-based MMR filter.

Triple notches can be achieved by integrating the folded EBG with a hollow T-shaped stub-based fundamental ultrawideband bandpass filter. This design is both straightforward and adaptable, effectively blocking unwanted narrow-band radio signals in the band and out of the band that may interfere with UWB operations while achieving high selectivity and compact size.

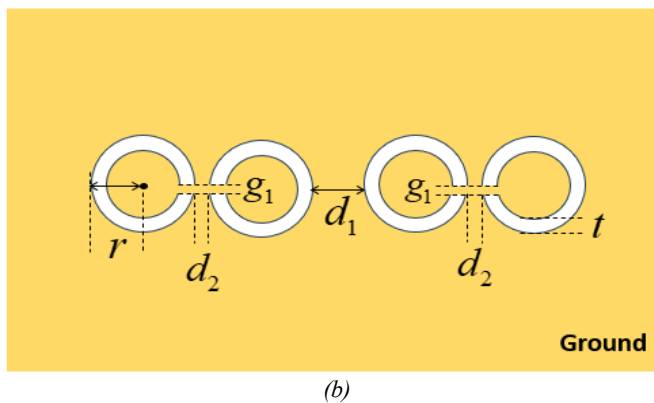
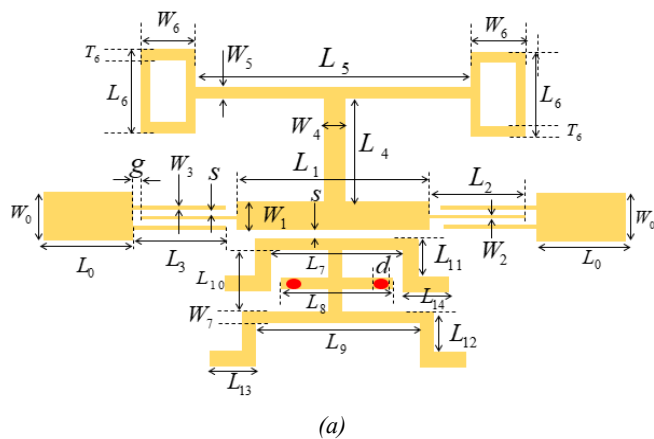


**Figure 6.** The structure of the proposed triple notched band BPF (a) top layer (b) bottom layer

## 4. RESULTS AND DISCUSSION

The design and optimization of the triple-notched ultrawideband bandpass filter (UWB BPF) were performed using the commercial software package Ansoft HFSS 2021. A Rogers 5880 substrate with a dielectric constant ( $\epsilon_r$ ) of 2.2, a loss tangent of 0.0009, and thickness  $h=0.51$  mm. Figure 7 depicts the simulated results of the proposed filter, indicating its high performance. The optimized dimensions for the filter are given in table 2 and the dimensions of the designed filter are approximately  $0.37 \lambda_g \times 0.95 \lambda_g$ .

**Table 2. Optimal Parameters of the Proposed Triple Notched Filter (all values in mm)**

Parameter	Value	Parameter	Value	Parameter	Value
L0	8.1	L3	8.2	L6	4.39
W0	1.64	W3	0.21	W6	2.14
L1	14	L4	3.87	t6	0.55
W1	1.8	W4	1.11	S	0.1
L2	8.26	L5	11.76	g	0.26
W2	0.25	W5	0.55	d	0.4
L7	9.4	L8	3.8	L10	2
W7	0.5	L9	8.6	L11	1
L12	1	L13	1.5	L14	1.5
d1	0.2	g1	0.2	t1	0.2
d2	0.5	r	1.2		

Based on the data acquired, the notched bands are visible at 4.93 GHz, 6.32 GHz, and 9.81 GHz, to mitigate interferences from IEEE 802.11j and IEEE 802.11be WLAN signals and X- band satellites communication systems (SCS). Rejection levels of the first, second and third notch are  $S_{21} < -18.8$  dB,  $S_{21} < -20.97$  dB, and  $S_{21} < -23.88$  dB, respectively. The return losses for the first, second, and third notched bands are observed at less than 1.2 dB ( $S_{11} > -1.2$  dB). The filter has a high selectivity; a 30 dB skirt factor of 0.91 and a 3 dB relative bandwidth for the notches of 5.5% for the first notch, 4.8% for the second notch, and 11.8% for the third notch, showing a sharp selectivity. Additionally, an upper stopband of less than 18 dB ( $S_{21} < -18$  dB) from 11 GHz up to 19.8 GHz is observed, where the most part is below 20dB. The group delay (GD) within the passband is measured between 0.32 ns and 1 ns, except at the notches, as indicated in figure 7. A comparison of the efficiency of the previously reported UWB filters with that of the proposed design is presented in table 3.

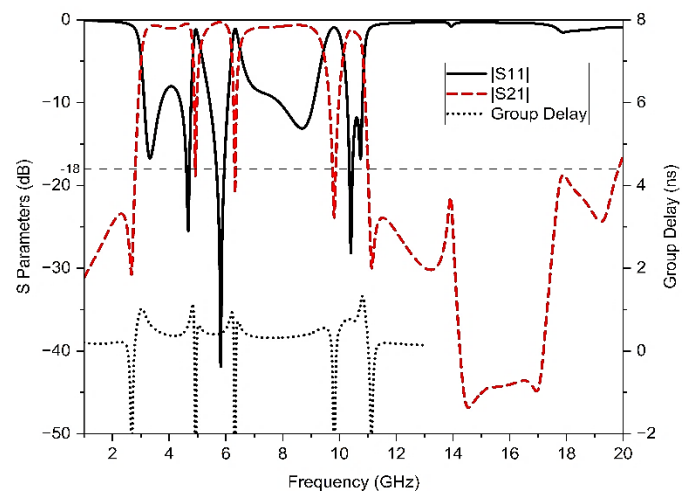


**Figure 7.** Simulation results of the proposed filter

**Table 3. Efficiency Comparison with Previous Studies**

Ref.	PB (GHz)	High S.F.?	IL (dB)	USB (GHz/dB)	NF/Att. (GHz/dB)	Size ( $\lambda_g \times \lambda_g$ )
[19]	2.8-10.6	No	0.8	NA	3.3,5.1,8.3/>15	0.06 x 0.02
[20]	3.25-10.73	Yes	0.52	16.9/>20	5.6,6.4,8.03/15	1.04 x 0.66

[12]	2.86-10.72	Yes	0.97	15.2/20	6,6.53,8.35/>15	0.81 x 0.71
[21]	2.75-10.7	Yes	<1.8	18/>15	6.1,8.1/>15.5	0.44 x 0.33
[22]	2.9-11.02	No	1	25/10	5/40	0.62 x 0.42
[23]	3.06-9.58	No	<1.5	13.47/20	5.48,7.68,8.82/>16	1.02 x 0.34
<b>This study</b>	<b>3.06-10.79</b>	<b>Yes</b>	<b>&lt;1.2</b>	<b>19.8/18</b>	<b>4.93,6.32,9.81/&gt;18</b>	<b>0.37 x 0.95</b>

The excellent frequency selectivity of 0.91 is attributed to the two transmission zeros positioned at 2.68 GHz and 11.14 GHz, which are created by the hollow T-shaped stub at the center of the design. By employing the CCSRR, the upper stopband was extended, and by employing the EBG structure, three notches were generated within the UWB passband. Therefore, our design achieves all the desired characteristics of the UWB passband, including good performance in the passband and upper stopband, high selectivity, and compact size with sharply notched bands.

## 5. CONCLUSION

This study proposes a high-performance UWB bandpass filter that employs a hollow T-shaped structure, metamaterial structure, and folded EBG structure to boost its performance. The incorporation of hollow T-shaped stubs introduces two transmission zeros at the lower and upper cutoff frequencies of 2.68 GHz and 11.14 GHz, significantly improving filter selectivity up to 0.91, and the implication of metamaterial structure extends the upper stop band up to 19.8 GHz with S21 lower than -18dB. In addition, the design contains a notch-band structure using a folded EBG architecture that permits the production of three notched bands. These notched bands can be easily tuned to certain frequencies by modifying the EBG-resonator settings. Spanning a frequency range from 3.06 GHz to 10.79 GHz, the proposed UWB bandpass filter successfully reduces interference from wireless bands as well as X-band satellite communication systems. The simplicity and flexibility of EBG make it an ideal solution for minimizing narrowband interference in UWB systems. Overall, the proposed planar UWB bandpass filter is appropriate for modern UWB wireless communication systems because it provides a compact design and excellent performance.

**Abbreviations:** Ref: reference, PB: passband, SF: selectivity factor, IL: insertion loss, USB: upper stopband, NF: notch frequency, Att: attenuation, NA: not applicable

## REFERENCES

- [1] A. Alarifi et al., "Ultra wideband indoor positioning technologies: Analysis and recent advances," *Sensors* (Switzerland), vol. 16, no. 5, pp. 1–36, 2016, doi: 10.3390/s16050707.
- [2] S. P.S., S. Vijay, and S. M., "Ultra-Wideband Technology: Standards, Characteristics, Applications," *Helix*, vol. 10, no. 4, pp. 59–65, 2020, doi: 10.29042/2020-10-4-59-65.
- [3] P. P. Shome, T. Khan, S. K. Koul, and Y. M. M. Antar, "Two Decades of UWB Filter Technology: Advances and Emerging Challenges in the Design of UWB Bandpass Filters," *IEEE Microw. Mag.*, vol. 22, no. 8, 2021, doi: 10.1109/MMM.2021.3078040.
- [4] R. P. Verma, B. Sahu, and A. Gupta, "Four-Stages Stepped-Impedance Resonator based Ultra-wideband Bandpass Filter with Tunable Notches," 2022 8th Int. Conf. Signal Process. Commun., pp. 121–124,

- 2022, doi: 10.1109/icsc56524.2022.10009503.
- [5] M. Y. Shavakand and J. Ahmadi-Shokouh, "Compact UWB filter with narrow notched band based on grounded circular patch resonator," *Int. J. Ultra Wideband Commun. Syst.*, vol. 4, no. 1, pp. 16–21, 2019, doi: 10.1504/IJUWBCS.2019.101173.
- [6] H. Bohra, A. Ghosh, A. Bhaskar, and A. Sharma, "A miniaturized notched band microstrip wideband filter with hybrid defected ground structure technique," *Proc. 3rd Int. Conf. Smart Syst. Inven. Technol. ICSSIT 2020*, no. Iessit, pp. 745–750, 2020, doi: 10.1109/ICSSIT48917.2020.9214245.
- [7] G. M. Yang, R. Jin, C. Vittoria, V. G. Harris, and N. X. Sun, "Small Ultra-wideband (UWB) bandpass filter with notched band," *IEEE Microw. Wirel. Components Lett.*, vol. 18, no. 3, pp. 176–178, 2008, doi: 10.1109/LMWC.2008.916781.
- [8] Y. Song, G.-M. Yang, and W. Geyi, "Compact UWB band-pass filter with dual notched bands based on novel defected ground structures," *IEEE Microw. Wirel. Components Lett.*, vol. 24, no. 4, pp. 230–232, 2014, doi: 10.1109/LMWC.2013.2296291.
- [9] F. Wei, L. Chen, Q. Y. Wu, X. W. Shi, and C. J. Gao, "Compact UWB bandpass filter with narrow notch-band and wide stop-band," *J. Electromagn. Waves Appl.*, vol. 24, no. 7, pp. 911–920, 2010, doi: 10.1163/156939310791285155.
- [10] J. Liu, W. Ding, J. Chen, and A. Zhang, "New ultra-wideband filter with sharp notched band using defected ground structure," *Prog. Electromagn. Res. Lett.*, vol. 83, no. April, pp. 99–105, 2019, doi: 10.2528/PIERL18111302.
- [11] M. Mirzaee and B. S. Virdee, "UWB bandpass filter with notch-band based on transversal signal-interaction concepts," *Electron. Lett.*, vol. 49, no. 6, pp. 379–399, 2013, doi: 10.1049/el.2012.4203.
- [12] P. Chakraborty, P. P. Shome, J. R. Panda, and A. Deb, "Highly Selective UWB Bandpass Filter with Multi-Notch Characteristics Using Comb Shaped Resonator," *Prog. Electromagn. Res. M*, vol. 108, no. November 2021, pp. 89–101, 2022, doi: 10.2528/PIERM21112601.
- [13] X. Zheng and T. Jiang, "Triple notches bandstop microstrip filter based on archimedean spiral electromagnetic bandgap structure," *Electron.*, vol. 8, no. 9, 2019, doi: 10.3390/electronics8090964.
- [14] G. Zhao, M. Li, R. Zhao, Z. Tu, Y. Yan, and X. Mo, "Highly Selective UWB Bandpass Filter with Dual Notch Bands Using Stub Loaded Multiple-mode Resonator," *Prog. Electromagn. Res. Symp.*, vol. 2021-Novem, pp. 1299–1309, 2021, doi: 10.1109/PIERS53385.2021.9695010.
- [15] P. Velez, J. Munoz-Enano, A. Ebrahimi, J. Scott, K. Ghorbani, and F. Martin, "Step impedance resonator (SIR) loaded with complementary split ring resonator (CSRR): Modeling, analysis and applications," *IEEE MTT-S Int. Microw. Symp. Dig.*, vol. 2020-Augus, pp. 675–678, 2020, doi: 10.1109/IMS30576.2020.9223926.
- [16] A. M. Albishi, M. K. E. Badawe, V. Nayyeri, and O. M. Ramahi, "Enhancing the sensitivity of dielectric sensors with multiple coupled complementary split-ring resonators," *IEEE Trans. Microw. Theory Tech.*, vol. 68, no. 10, pp. 4340–4347, 2020, doi: 10.1109/TMTT.2020.3002996.
- [17] R. Selvaraju, M. H. Jamaluddin, M. R. Kamarudin, J. Nasir, and M. H. Dahri, "Complementary split ring resonator for isolation enhancement in 5G communication antenna array," *Prog. Electromagn. Res. C*, vol. 83, no. April, pp. 217–228, 2018, doi: 10.2528/pierc18011019.
- [18] F. Wei, W. T. Li, X. W. Shi, and Q. L. Huang, "Compact UWB bandpass filter with triple-notched bands using triple-mode stepped impedance resonator," *IEEE Microw. Wirel. Components Lett.*, vol. 22, no. 10, pp. 512–514, 2012, doi: 10.1109/LMWC.2012.2215845.
- [19] A. Basit, M. I. Khattak, and M. Al-Hasan, "Design and Analysis of a Microstrip Planar UWB Bandpass Filter with Triple Notch Bands for WiMAX, WLAN, and X-Band Satellite Communication Systems," *Prog. Electromagn. Res. M*, vol. 93, pp. 155–164, 2020, doi: 10.2528/PIERM20042602.
- [20] M. Sazid and N. S. Raghava, "Planar UWB-bandpass filter with multiple passband transmission zeros," *Int. J. Electron. Communications*, vol. 134, 2021, doi: https://doi.org/10.1016/j.aeeu.2021.153711.
- [21] A. N. Ghazali, M. Sazid, and S. Pal, "A miniaturized low-cost microstrip-to-coplanar waveguide transition-based ultra-wideband bandpass filter with multiple transmission zeros," *Microw. Opt. Technol. Lett.*, vol. 62, no. 12, pp. 3662–3667, 2020, doi: 10.1002/mop.32482.
- [22] P. Kumari, P. Sarkar, and R. Ghatak, "A multi-stub loaded compact UWB BPF with a broad notch band and extended stopband characteristics," *Int. J. RF Microw. Comput. Eng.*, vol. 30, no. 4, pp. 1–

8, 2020, doi: 10.1002/mmce.22138.

- [23] P. Chakraborty, J. R. Panda, A. Deb, S. Sahu, and J. S. Roy, "Design of a Miniaturized Split-Ring Resonator Based UWB Notched Bandpass Filter," *Prog. Electromagn. Res. C*, vol. 134, no. June, pp. 27–38, 2023, doi: 10.2528/PIERC23050801.



© 2025 by Richard Patience Shema, Dominic B. O. Konditi and Elijah Mwangi. Submitted for possible open access publication under the terms and conditions of the Creative Commons Attribution (CC BY) license (<http://creativecommons.org/licenses/by/4.0/>).